Kramers–Kronig analysis of infrared reflection spectra with perpendicular polarization

Kiyoshi Yamamoto, Akio Masui, and Hatsuo Ishida

The application of Kramers–Kronig analysis for reflection spectra from a single interface with perpendicular (s) polarization has been studied theoretically with regard to a phase correction term. The errors in phase shift and complex refractive index obtained by the use of Kramers–Kronig analysis have been examined for such techniques as external, internal, and total internal reflection spectroscopies by the use of spectral simulation and the complex refractive index based on dispersion theory. The advantages and disadvantages of the various measurement techniques used to obtain the complex refractive index of a sample material have been compared. It is concluded that the external reflection technique can be used until the sample thickness becomes too thin to provide the edge shape necessary to avoid the detection of reflection from the back surface. The total internal reflection technique should be used only for a thin-film sample because knowledge of the refractive index at some frequency is required and because this technique may yield larger errors than the other techniques in the complex refractive index obtained by the use of Kramers–Kronig analysis.

Introduction

Kramers–Kronig analysis of an infrared (IR) transmission spectrum has been applied to extract the complex refractive index of film materials.[1–5] Because this technique involves the use of the Hilbert transformation from the imaginary part to the real part of a complex refractive index, $\hat{n}$,[6] n_∞ (the refractive index at a frequency without absorption in the visible region) is always required. Moreover, both parts of $\hat{n}$ cannot be directly observed, so an iteration procedure, for which the observed spectrum is used as an initial value, is essential in addition to the film thickness. The same algorithm has also been used for Kramers–Kronig analysis of attenuated total reflection (ATR) spectrum, where the thickness value is not required.[7–11] Because the distortion of the observed spectrum depends on the absorption (dispersion), the refinement procedure may diverge for strong absorption for which the extinction coefficient is more than ~ 0.8.[11] Sample preparation to produce thin films that show adequate transmissivity is also difficult for materials that have a strong absorption in transmission.

On the other hand, Kramers–Kronig analysis for a reflection spectrum from a single interface has often been used to obtain a complex refractive index[12–13] since it was applied to polethylene by Robinson.[12–31] Because this technique uses the Hilbert transformation from the real part to the imaginary part in the logarithm of the complex reflectivity, $\ln \hat{r}$,[6] n_∞ is not always necessary, as is shown below. The real part of the complex reflectivity is directly measured as the energy reflectivity, so that the iteration procedure is not necessary. Because this method requires reflection data for the entire frequency range from $\nu = 0$ to ∞, extrapolation methods have been investigated.[15,22,28] Furthermore, several studies have been done to extend this method to more general cases, such as reflection through a transparent window with refractive index $n_0 > 1$ and reflection at an oblique angle of incidence.[14,21,23,24] To obtain the complex refractive index in these cases, it has been shown that a correction term is necessary for the phase shift of the reflection. This correction term has been derived by considering the integration path for which the singularities on the imaginary axis in the complex plane are avoided. Taking account of this correction term,

When this research was performed, K. Yamamoto and H. Ishida were with the Department of Macromolecular Science, Case Western Reserve University, Cleveland, Ohio 44106-7202. A Masui is with the Research Center, Asahi Glass Company, Ltd., 1150 Hazawa, Kanagawa-ku, Yokohama 221, Japan. K. Yamamoto is now with the Research Center, Asahi Glass Company, Ltd.

Received 19 November 1992; revised manuscript received 18 March 1994.

0003-6935/94/276285-09$06.00/0.

Bardwell and Dignam[25] determined the complex refractive index of some organic liquid materials by Kramers–Kronig analysis of the ATR spectra with s polarization.

Recently Kramers–Kronig analysis of the ATR spectrum has often been used to extract the complex refractive index, especially for liquid materials, because an optically flat surface is easily obtained and the thickness value, which is required for transmission, is not necessary.[7–11,26,29] However, an examination of which measurement technique is appropriate to obtain the complex refractive index and what the magnitude of errors yielded in the complex refractive index obtained by Kramers–Kronig analysis has not been performed.

The purpose of this paper is to describe the phase correction terms in detail for practical measurement techniques with s polarization. The validity of these correction terms is checked with spectral simulation and a noise-free complex refractive index derived from dispersion theory. The advantages and disadvantages of the various measurement techniques in obtaining the complex refractive index are also compared.

Calculation Methods

In this paper only the s polarization for which the electric vector is perpendicular to the incident plane is considered with the optical configuration shown in Fig. 1. For this situation there is only a single interface; therefore the complex reflectivity for the s polarization, $\hat{r}_s$, is simply given by the Fresnel equation.[32]

$$\hat{r}_s = \frac{n_0 \cos\theta_0 - \hat{n}_1 \cos\hat{\theta}_1}{n_0 \cos\theta_0 + \hat{n}_1 \cos\hat{\theta}_1}. \tag{1}$$

Although there exists another definition in which the sign of $\hat{r}_s$ is different from that in this paper, Eq. (1) is adopted here. Using the energy reflectivity for the s polarization, R_s, we express $\hat{r}_s$ as follows:

$$\hat{r}_s = \sqrt{R_s}\exp(i \cdot \delta_s), \tag{2}$$

where δ_s is the phase shift of the reflection for s polarization. Here δ_s is defined as $-\pi \le \delta_s < \pi$.

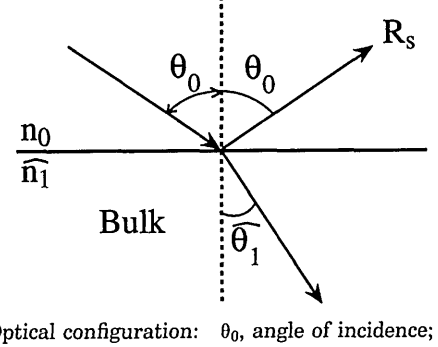

Fig. 1. Optical configuration: θ_0, angle of incidence; n_0, refractive index of the incident media; $\hat{n}_1$, complex refractive index of the sample material; R_s, energy reflectivity in s polarization.

On the other hand the reflection spectrum is simulated as the energy reflectivity from the known complex refractive index with Eqs. (1) and (3).

$$R_s = |\hat{r}_s|^2. \tag{3}$$

Phase Correction Term

The phase correction term for Kramers–Kronig analysis of reflection spectra has been given in the practical form by Bardwell and Dignam.[25,26,30] The sign of the correction terms depends on the definition of the direction of the reflected electric vector. Because the derivation of the correction term is helpful for understanding its nature, a detailed derivation of the correction term is given below.

To obtain the Kramers–Kronig relationship with respect to the reflection, the logarithm of Eq. (2) is taken.

$$\ln \hat{r}_s = \ln\sqrt{R_s} + i\delta_s. \tag{4}$$

By applying the Hilbert transformation from the real part to the imaginary part in Eq. (4), the Kramers–Kronig relationship is obtained.[6]

$$\delta_s^{KK}(\nu') = -\frac{\nu'}{\pi}\int_0^\infty \frac{\ln R_s(\nu) - \ln R_s(\nu')}{\nu^2 - \nu'^2}\,d\nu. \tag{5}$$

Although there are different forms of the Kramers–Kronig relationship for reflection,[14,17,18] Eq. (5) is the most convenient form for the calculation because this function does not diverge even when $\nu = \nu'$.[31] However, Eq. (5) does not include the phase shift that is due to the singularities on the imaginary axis in the complex plane, that is, the points where $R_s = 0$.[14] Taking this into account, we obtain the actual phase shift, δ_s^{act}, as follows:

$$\delta_s^{act} = \delta_s^{KK} + \delta_s^{corr}, \tag{6}$$

where δ_s^{corr} is the phase correction term. From Eq. (5), it is obvious that δ_s^{KK} equals 0 for frequencies with no absorption. This fact is compared with the phase shift δ_s calculated from Eq. (1), assuming no absorption, so that δ_s^{corr} is obtained as δ_s for this situation. The difference between δ_s and δ_s^{act} is assigned to the errors in Kramers–Kronig analysis and to uncertainty in the phase correction.

Now Snell's law is expressed as follows:

$$n_0 \sin\theta_0 = \hat{n}_1 \sin\hat{\theta}_1. \tag{7}$$

Because a frequency at which there is no absorption is considered here, the extinction coefficient k_1 is equal to 0; therefore the refractive index of the sample, n_1, is used instead of the complex refractive index $\hat{n}_1$, because $\hat{n}_1 = n_1 + ik_1$. From Eq. (7) two conditions must be considered: one is $\sin\hat{\theta}_1 < 1$, $\hat{\theta}_0 < 90°$ for $n_0 < n_1$ and $\theta_0 < \theta_c$ for $n_0 > n_1$, and the other is $\sin\theta_1 > 1$, i.e., $\theta_0 > \theta_c$ for $n_0 > n_1$, where $\theta_c = \sin^{-1}(n_1/n_0)$ is the critical angle of incidence. For the first condition it is obvious that the angle of

Table 1. Phase Correction Term of the Kramers–Kronig Analysis for the Reflection in s Polarization

Case	Condition	Phase Correction Term (δ_s^{corr})[a]	Remark
(A)	$n_0 < n_1$	$-\pi$	External reflection
(B)	$n_0 > n_1, \theta_0 < \theta_c$	0	Internal reflection
(C)	$n_0 > n_1, \theta_0 > \theta_c$	$2\tan^{-1}\left[\frac{(n_0^2 \sin^2\theta_0 - n_1^2)^{1/2}}{n_0 \cos\theta_0}\right] - \pi$	Total internal reflection

[a]Actual phase correction term $\delta_s^{act} = \delta_s^{KK} + \delta_s^{corr}$.

refraction is a real quantity, and the equation below is obtained from Eq. (7):

$$\cos\theta_1 = \left(1 - \frac{n_0^2}{n_1^2}\sin^2\theta_0\right)^{1/2}. \tag{8}$$

From Eqs. (1) and (8), we obtain

$$\hat{r}_s = \frac{n_0\cos\theta_0 - (n_1^2 - n_0^2\sin^2\theta_0)^{1/2}}{n_0\cos\theta_0 + (n_1^2 - n_0^2\sin^2\theta_0)^{1/2}} = \frac{(n_0 - n_1)(n_0 + n_1)}{[n_0\cos\theta_0 + (n_1^2 - n_0^2\sin^2\theta_0)^{1/2}]^2}. \tag{9}$$

Equation (9) shows that there is no imaginary part of $\hat{r}_s$, that $\hat{r}_s$ is a real quantity under the condition sin $\theta_1 < 1$, and that the sign of $\hat{r}_s$ depends on the term, $n_0 - n_1$. The point at which the sign of the $\hat{r}_s$ changes, $n_0 = n_1$, corresponds to the singularity on the imaginary axis of the complex plane.[14] Therefore two cases must be considered: $n_0 < n_1$ for case (A) and $n_0 > n_1$ for case (B). For case (A), $\hat{r}_s = -\sqrt{R_s} < 0$, following from our definition of $\hat{r}_s$. To solve this situation, the phase shift $-\pi$ is introduced.

$$\hat{r}_s = \sqrt{R_s}\exp[i(\delta_s^{KK} - \pi)]. \tag{10}$$

Then the phase correction term $\delta_s^{corr} = -\pi$ is necessary for this case. For case (B), the equation that follows is

$$\hat{r}_s = \sqrt{R_s}\exp(i\delta_s^{KK}). \tag{11}$$

Therefore no correction term is necessary.

For the second condition $\theta_0 > \theta_c$, denoted as case (C), cos $\hat{\theta}_1$ is purely imaginary, and the next equation is given instead of Eq. (8).

$$\cos\hat{\theta}_1 = i\left(\frac{n_0^2}{n_1^2}\sin^2\theta_0 - 1\right)^{1/2}. \tag{12}$$

From Eqs. (1) and (12),

$$\hat{r}_s = \frac{n_0\cos\theta_0 - i(n_0^2\sin^2\theta_0 - n_1^2)^{1/2}}{n_0\cos\theta_0 + i(n_0^2\sin^2\theta_0 - n_1^2)^{1/2}} = \frac{n_0^2\cos^2\theta_0 - n_0^2\sin^2\theta_0 + n_1^2 - 2n_0\cos\theta_0 i(n_0^2\sin^2\theta_0 - n_1^2)^{1/2}}{n_0^2 - n_1^2}. \tag{13}$$

Equation (13) shows that a phase shift has occurred even when no absorption is considered for the sample. The magnitude of the phase shift δ_s^{corr} is obtained in the following manner:

$$\delta_s^{corr} = \tan^{-1}\left(\frac{\mathrm{Im}\,\hat{r}_s}{\mathrm{Re}\,\hat{r}_s}\right) = \tan^{-1}\left[\frac{2n_0\cos\theta_0(n_0^2\sin^2\theta_0 - n_1^2)^{1/2}}{n_0^2 - n_1^2 - 2n_0^2\cos^2\theta_0}\right], \tag{14}$$

where Re and Im indicate real part and imaginary part, respectively. In Eq. (13), Im $\hat{r}_s$ is always negative, so δ_s^{corr} should be between $-\pi$ and 0. Therefore arctangent must be defined between $-\pi$ and 0 in Eq. (14). Using double-angle formulas, we can rewrite Eq. (14) as follows:

$$\delta_s^{corr} = 2\tan^{-1}\left[\frac{(n_0^2\sin^2\theta_0 - n_1^2)^{1/2}}{n_0\cos\theta_0}\right] - \pi, \tag{15}$$

where the function of arctangent is defined in a common way, that is, between $-\pi/2$ and $\pi/2$. Equation (15) is basically identical with the correction term given by Bardwell and Dignam.[25,26,30] The correction term for each case is summarized in Table 1.

Here it is mentioned again that these correction terms have validity only for *s* polarization, and the refractive index of the material must be known at least at a frequency without the absorption for case (C).

Table 2. Dispersion Parameters for the Complex Refractive Index of an Organic Model

ν_0 (cm^{-1})	1500
γ (cm^{-1})	20
ε_∞	2.25
$\varepsilon_\infty - \varepsilon_0$	0.015
n_∞	1.5
Spectrum range (cm^{-1})	1000–2000

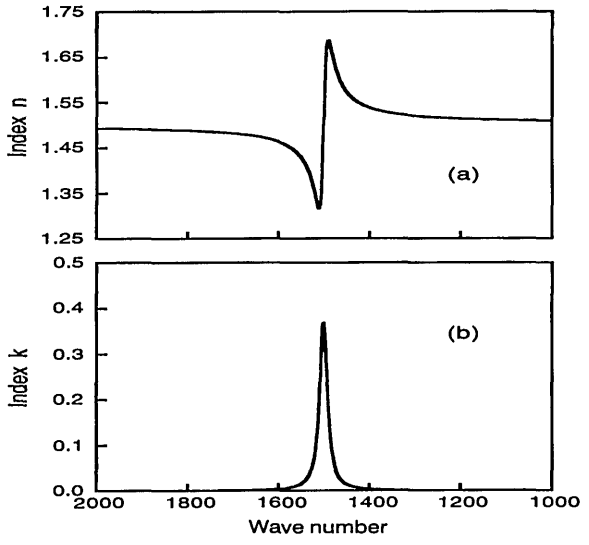

Fig. 2. Complex refractive index for the organic model: (a) real part, (b) imaginary part.

Combining Eqs. (1) and (7) yields Eq. (16) after simplification, which is used to calculate $\hat{n}_1$.

$$\hat{n}_1 = n_0\left[1 - \frac{4\hat{r}_s \cos^2 \hat{\theta}_0}{(1 + \hat{r}_s)^2}\right]^{1/2}. \tag{16}$$

The complex refractive index $\hat{n}_1$ can be calculated with Eqs. (2), (5), (6), and (16).

B. Complex Refractive Index Based on Dispersion Theory

The complex refractive index for a model material is derived from the dispersion theory.[33] For any transitions that include vibrational modes, the complex dielectric constant $\hat{\varepsilon}(\nu)$ is expressed as follows:

$$\hat{\varepsilon}(\nu) = \varepsilon_\infty - \frac{(\varepsilon_0 - \varepsilon_\infty)\nu_0^2}{\nu^2 + i\gamma\nu - \nu_0^2}, \tag{17}$$

where ε_0 and ε_∞ are the dielectric constants at $\nu = 0$ and ∞, respectively; γ is the damping constant for the oscillator; and ν_0 is the frequency of the proper vibration. There is the following relationship between the complex dielectric constant and the complex refractive index.

$$\mu\hat{\varepsilon}(\nu) = \hat{n}(\nu)^2, \tag{18}$$

where μ is a magnetic permeability and is equal to 1 in the optical region, so that Eq. (19) is obtained.

$$\hat{n}(\nu) = \sqrt{\hat{\varepsilon}(\nu)}. \tag{19}$$

Thus the noise-free complex refractive indices are

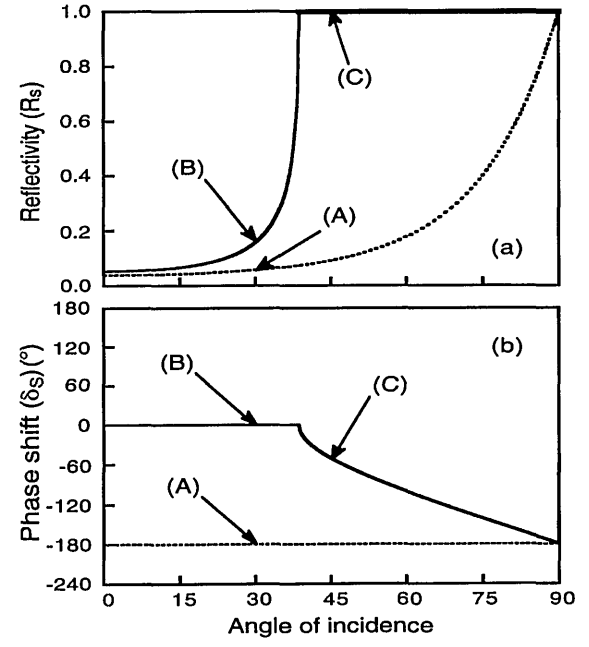

Fig. 3. Angle dependence of (a) the reflectivity and (b) the phase shift: solid curves, $n_0 = 2.4$, $n_1 = 1.5$; dashed curves, $n_0 = 1.0$, $n_1 = 1.5$. The points indicated by the arrows correspond to the conditions for cases (A)–(C).

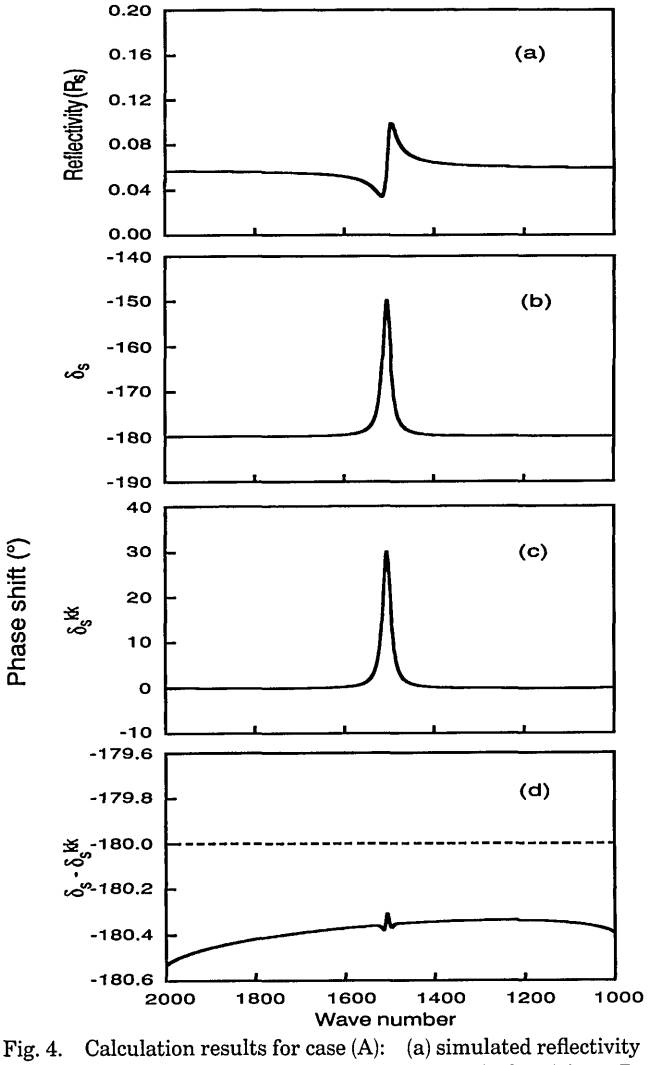

Fig. 4. Calculation results for case (A): (a) simulated reflectivity R_s; (b) simulated phase shift δ_s; (c) phase shift calculated from R_s with the Kramers–Kronig analysis, δ_s^{KK}; and (d) solid curve, difference $\delta_s - \delta_s^{KK}$; dashed line, phase correction term $\delta_s^{corr} = -180°$.

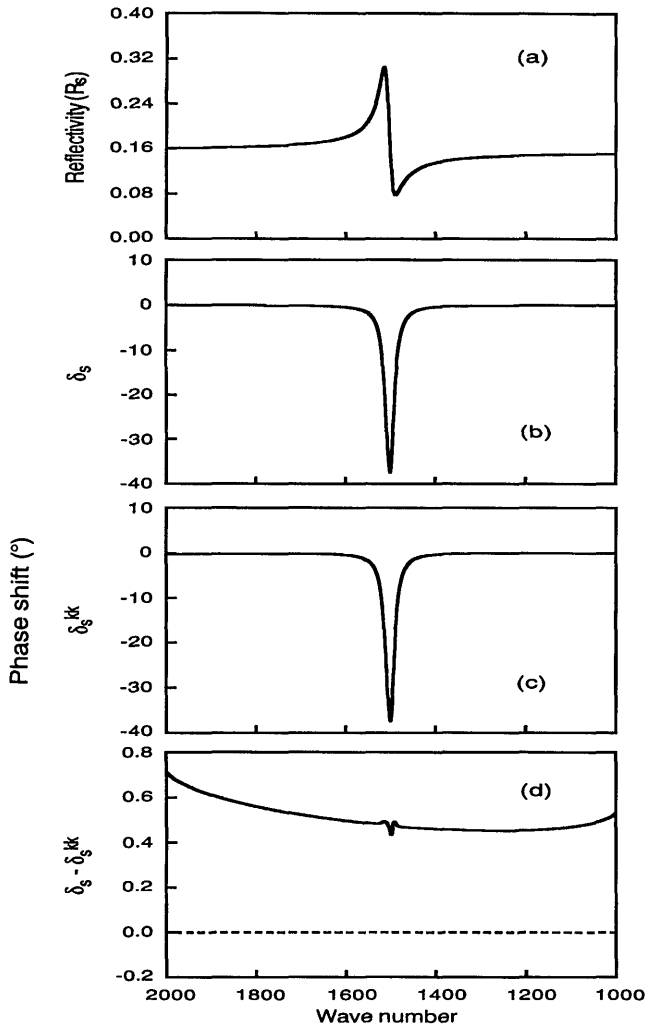

Fig. 5. Calculation results for case (B): (a) simulated reflectivity R_s; (b) simulated phase shift δ_s; (c) phase shift calculated from R_s by the Kramers–Kronig analysis, δ_s^{KK}; and (d) solid curve, difference $\delta_s - \delta_s^{KK}$; dashed line, phase correction term $\delta_s^{corr} = 0°$.

obtained from Eqs. (17) and (19) by assigning values to ε_0, ε_∞, γ, and ν_0.

There are Kramers–Kronig relationships between the real and the imaginary parts of $\hat{r}_s$, $\hat{\varepsilon}$, and $\hat{n}$ calculated from Eqs. (1), (17), and (19), respectively, because they satisfy causality.[6]

Experimental

The programs used in this paper have been written in FORTRAN 77, and all calculations have been done on a Micro VAX computer with the VMS operating system. The procedures of integration and extrapolation for the Kramers–Kronig analysis has been reported.[31]

Results and Discussion

To check the correction terms, the noise-free complex refractive index based on the dispersion theory is used as a model for an organic material. It has a moderate absorption for organic materials for which the dispersion parameters are listed in Table 2 and shown in Fig. 2. The spectrum range used in integration of Kramers–Kronig analysis is also shown in Table 2. This absorption has been assumed to be a carbonyl stretching band, although its peak position is at a slightly lower frequency. The optical conditions used in the calculations are, for the external reflection, $n_0 = 1.0$, $\theta_0 = 30°$, which is case (A); for internal reflection, $n_0 = 2.4$, $\theta_0 = 30°$, which is case (B); and for total internal reflection, $n_0 = 2.4$, $\theta_0 = 45°$, which is case (C). In practice, case (C) corresponds to the ATR experiment for absorbing media. The incident angle dependencies on the reflectivity R_s, calculated from Eqs. (3), (9), and (13), and the phase shift, δ_s, obtained from Table 1 for $n_0 = 1.0$, $n_1 = 1.5$, and $n_0 = 2.4$, and $n_1 = 1.5$, are shown in Fig. 3. $r_s = \sqrt{R_s}\exp(i\delta_s)$. Therefore R_s and δ_s correspond to the amplitude and the phase shift of the complex reflectivity $\hat{r}_s$. It can also be seen in Fig. 3 that only one of them (R_s or δ_s) changes with the angle of incidence and that the phase shift is constant below θ_c but is delayed over this angle and approaches $-\pi$ at $\theta_0 = 90°$. Each case corresponding to the points

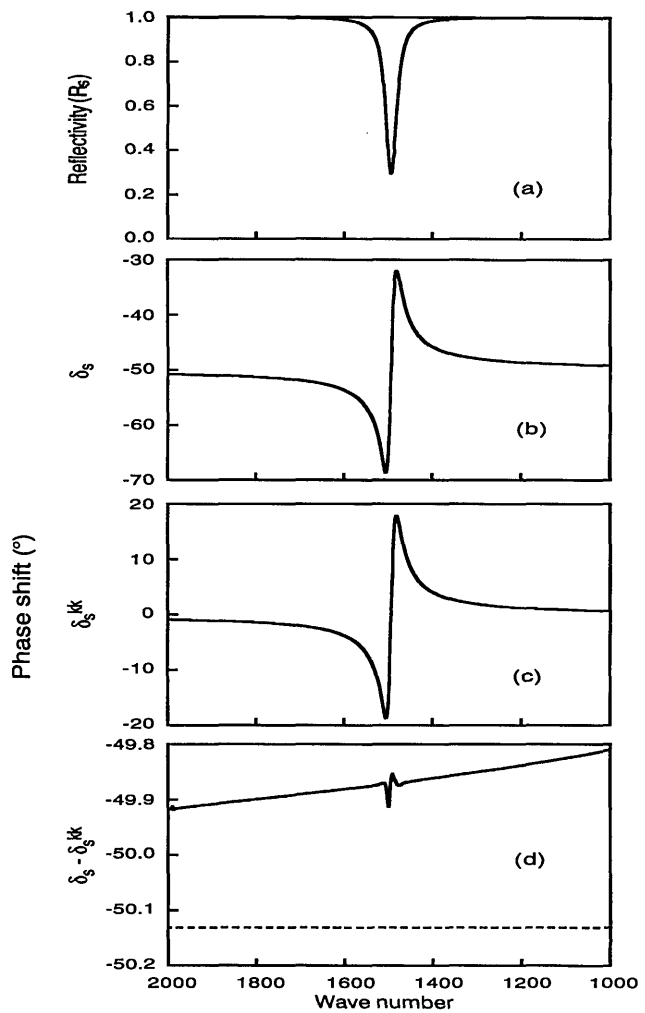

Fig. 6. Calculation results for case (C): (a) simulated reflectivity R_s; (b) simulated phase shift δ_s; (c) phase shift calculated from R_s by the Kramers-Kronig analysis δ_s^{KK}; and (d) curve, difference $\delta_s - \delta_s^{KK}$; dashed line, phase correction term $\delta_s^{corr} = -50.13°$.

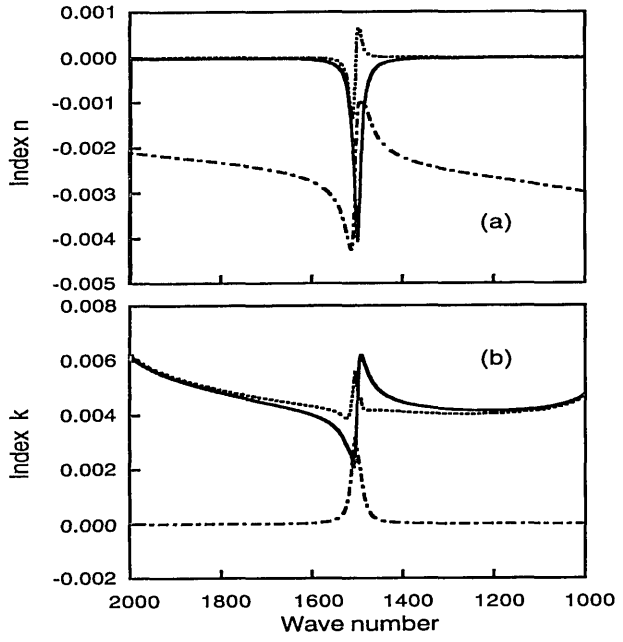

Fig. 7. Errors in the complex refractive index for the organic model: (a) real part, (b) imaginary part. Solid curves, case (A); dotted curves, case (B); dashed–dotted curves, case (C).

indicated in Fig. 3 is discussed in the following section.

For case (A), the simulated reflectivity R_s and the simulated phase shift δ_s are shown in Figs. 4(a) and 4(b), respectively. It is shown in Fig. 4(b) that the phase is affected when absorption occurs. The phase shift δ_s^{KK} calculated from the reflectivity R_s with the Kramers–Kronig relationship [Eq. (5)] is shown in Fig. 4(c). With the Kramers–Kronig analysis, the phase shift is estimated as ~0 for frequencies with no absorption. The difference $\delta_s - \delta_s^{KK}$ shown in Fig. 4(d) almost agrees with the phase correction term $\delta_s^{corr} = -180°$ for this case. The relatively small deviation, corresponding to approximately 1% of the phase shift for the absorption, may be caused by the integration and extrapolation in the Kramers–Kronig analysis.

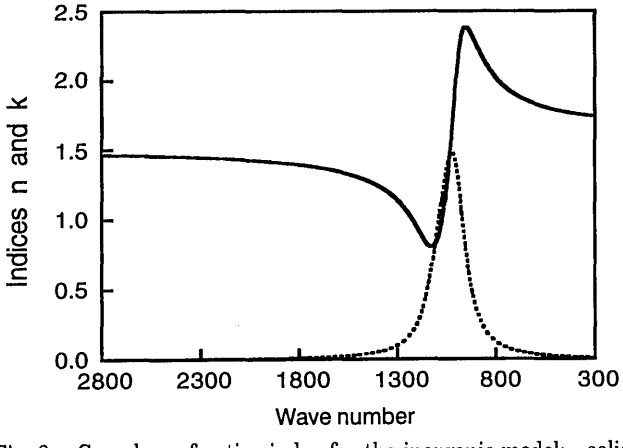

Fig. 8. Complex refractive index for the inorganic model: solid curve, real part; dotted curve, imaginary part.

Table 3. Dispersion Parameters for the Complex Refractive Index of an Inorganic Model

ν_0 (cm^{-1})	1000
γ (cm^{-1})	125
ε_∞	2.25
$\varepsilon_\infty - \varepsilon_0$	0.7
n_∞	1.5
Spectrum range (cm^{-1})	300–2800

For case (B), the calculated results shown in Fig. 5 are obtained in the same manner as for case (A). In this case the phase shift is delayed contrary to case (A) when absorption occurs. The difference $\delta_s - \delta_s^{KK}$ shown in Fig. 5(d) nearly agrees with the phase correction term $\delta_s^{corr} = 0°$.

For case (C), the calculation results are shown in Fig. 6 in the same manner as for cases (A) and (B). The reflectivity at the frequency with no absorption is 1; i.e., the total internal reflection condition makes the extrapolation required in the Kramers–Kronig analysis easier. The phase shift has a minimum and maximum, contrary to cases (A) and (B). The difference $\delta_s - \delta_s^{KK}$ shown in Fig. 6(d) is in fairly good agreement with the correction term $\delta_s^{corr} = -50.13°$ calculated from Eq. (15) for $n_0 = 2.4$ and $n_1 = 1.5$. The offset between $\delta_s - \delta_s^{KK}$ and δ_s^{corr} is caused by the difference between the refractive index n_1 at any frequency and the refractive index used in the phase correction term calculation, i.e., n_∞ in this case, in addition to the integration in the Kramers–Kronig analysis. If n_1 is known at any frequency, the offset can be reduced. Furthermore, there is the slope in

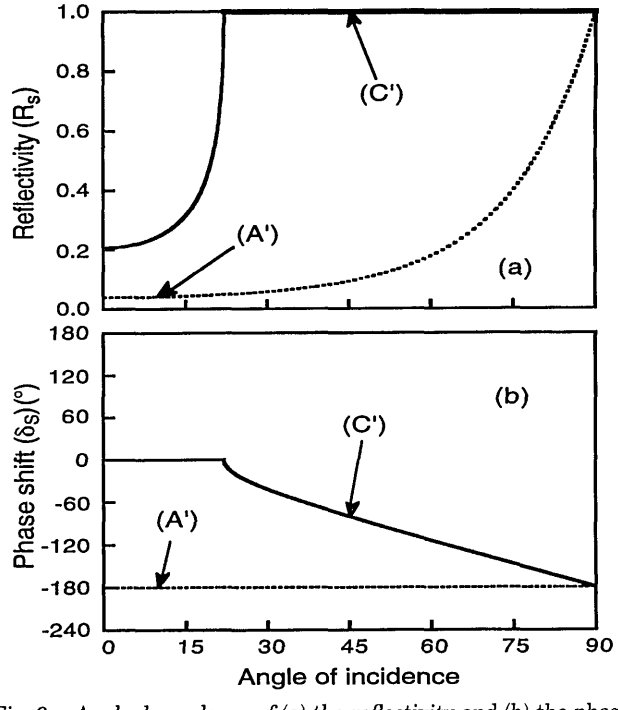

Fig. 9. Angle dependence of (a) the reflectivity and (b) the phase shift: solid curves, $n_0 = 4.0$, $n_1 = 1.5$; dotted curve and line, $n_0 = 1.0$, $n_1 = 1.5$. The points indicated by the arrows correspond to the conditions for cases (A') and (C').

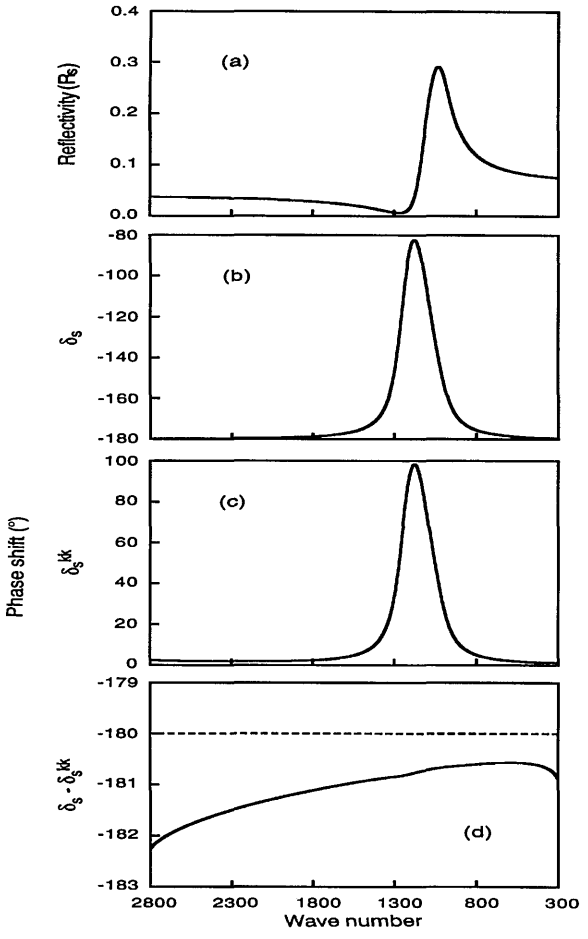

Fig. 10. Calculation results for case (A′): (a) simulated reflectivity R_s; (b) simulated phase shift δ_s; (c) phase shift calculated from R_s by the Kramers–Kronig analysis, δ_s^{KK}; and (d) solid curve, difference $\delta_s - \delta_s^{KK}$; dotted line, phase correction term $\delta_s^{corr} = -180°$.

$\delta_s - \delta_s^{KK}$ that is due to the difference between ε_∞ and ε_0. In practice it can be ignored for an organic material because the slope is small. However, this effect may not be neglected for an inorganic material because of the material's large $(\varepsilon_\infty - \varepsilon_0)$.[24] This is discussed below.

The error in the complex refractive index, i.e., the difference between the refractive index of the organic model and the refractive index calculated from R_s and $\delta_s^{KK} + \delta_s^{corr}$ for each case is shown in Fig. 7. Although the error is the smallest for case (B), the results for all cases are small enough to obtain the complex refractive index of the organic material accurately.

To check the validity of these methods for an inorganic material, a stronger absorption ($k_{max} \geq 1.5$), shown in Fig. 8, is considered as the model of silicate glasses, and the dispersion parameters and spectrum range are listed in Table 3. The optical conditions used in the calculation are external reflection $n_0 = 1.0$ and $\theta_0 = 10°$ for case (A′) and total internal reflection, $n_0 = 4.0$, $\theta_0 = 45°$ for case (C′) (see Fig. 9). Because the inorganic model shows absorption that is too strong under conditions for case (C), the optical condition is different from that of the organic model. The incident angle dependence on the reflectivity R_s and the phase shift δ_s in Fig. 9 are calculated for case (A′) and (C′) in the same manner as in Fig. 3.

For cases (A′) and (C′), the calculation results shown in Figs. 10 and 11, respectively, are obtained in the same manner as for the cases (A) and (C). The difference $\delta_s - \delta_s^{KK}$ for case (A′) is closer to δ_s^{corr} than for case (C′), and the ratio of $\delta_s - \delta_s^{KK}$ over the change of the δ_s or δ_s^{KK} is smaller for case (A′) than for case (C′). This is clearer in Fig. 12, which shows the error in the complex refractive index, i.e., the difference between the complex refractive index of the inorganic model and the complex refractive index calculated from R_s and $\delta_s^{KK} + \delta_s^{corr}$ for each case. The error is obviously smaller in case (A′). These errors correspond to approximately 1% and 10% of the original complex refractive index for cases (A′) and (C′), respectively. This difference is due to the fact that ε_∞ and ε_0 are evaluated from the reflectivity

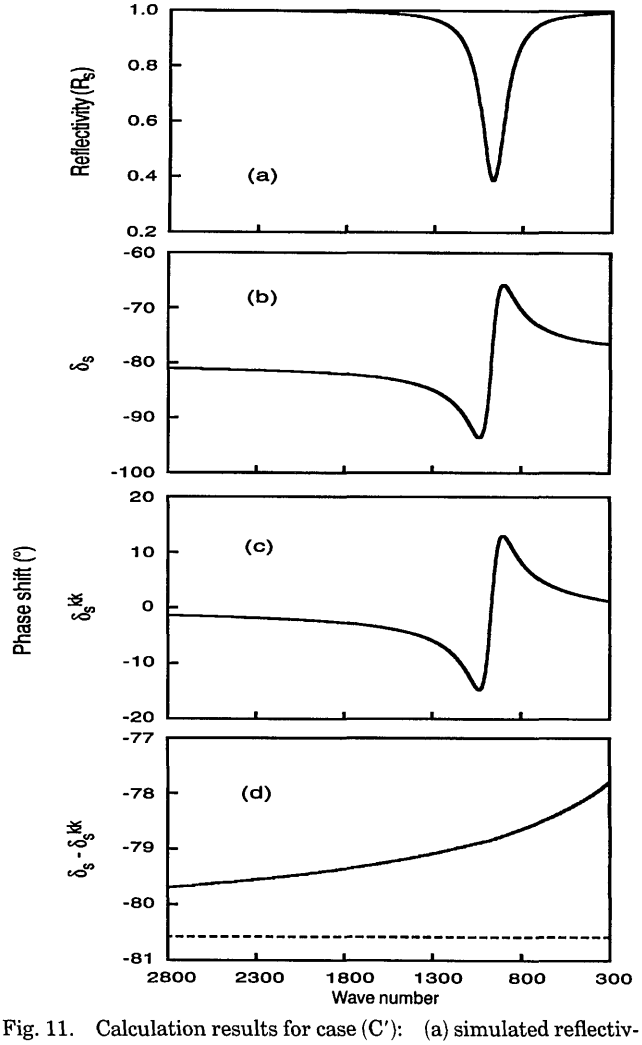

Fig. 11. Calculation results for case (C′): (a) simulated reflectivity R_s; (b) simulated phase shift, δ_s; (c) phase shift calculated from R_s by the Kramers–Kronig analysis, δ_s^{KK}; and (d) difference $\delta_s - \delta_s^{KK}$ and phase correction term $\delta_s^{corr} = -80.58°$.

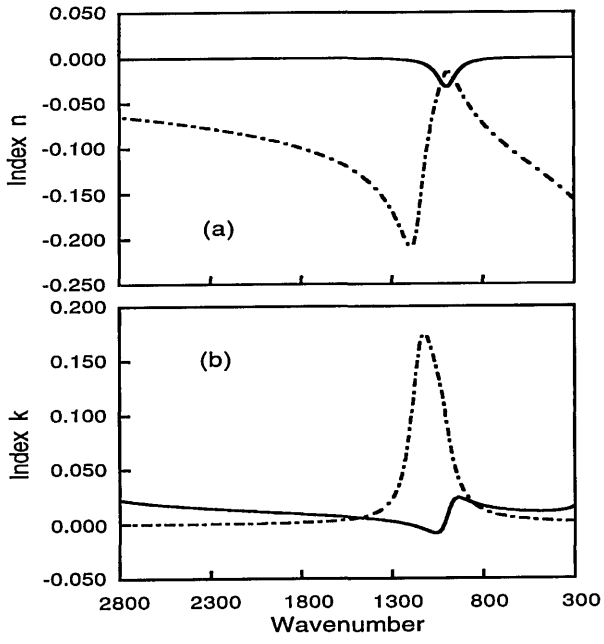

Fig. 12. Errors in the complex refractive index for the inorganic model: (a) real part, (b) imaginary part. Solid curves, case (A'); dash–dotted curves, case (C').

R_s at the frequencies above and below the absorption peak, respectively, for case (A') (external reflection), although not for case (C') (total internal reflection). This situation can be improved, especially for case (C'), if some anchor points (the refractive indices at some frequencies without absorption) are known.

Conclusions

In this paper the errors of the Kramers–Kronig analysis in some practical measurement techniques have been studied as well as the phase correction terms for reflection. For an organic material, the external, internal, and total internal reflection experiments can be used to obtain the complex refractive index. Among these techniques, only total internal reflection can be applied to a film sample. However, its use requires the knowledge of n_1 at some frequency, which is a big disadvantage of this technique. The greatest advantage of the other techniques is that they do not need n_1 to obtain this complex refractive index. However, the reflection from the back surface of the sample must be avoided in these techniques,[34] which may limit the application of these techniques in terms of sample shape. The internal reflection technique may be a better technique than the total internal reflection technique, which has often been used[7–11,26,29] to obtain the complex refractive index of a liquid sample because the n_1 of the sample is not necessary. Another advantage is that a completely flat surface can be easily obtained, similar to the case of total internal reflection, but the measurement of the background spectrum is more difficult. This problem may be solved by the use of a metal deposited on a prism as a reference. For nonvolatile liquid materials, external reflection can be the best technique because the reflection spectra can be observed from the free surface and, again, the n_1 of the sample is not necessary.

For an inorganic material there is a large error, ~10%, in the complex refractive index obtained from the total internal reflection, whereas the error is ~1% from the external reflection. The external reflection technique should be used unless the sample is too thin to obtain the edge shape necessary to avoid the detection of reflection from back surface, because the total internal reflection technique requires the knowledge of n_1 at some frequency and leads to a fairly large error. The error may be reduced if multiple anchor points are used. Furthermore, no internal reflection element allows one to determine the complex refractive index in the far-infrared region, where the most of absorptions occurs for inorganic materials.

To avoid the detection of reflection from back surface even for Kramers–Kronig analysis of ATR spectra, the sample must be sufficiently thicker than penetration depth (usually more than several micrometers). For thinner film materials, some modification is necessary for Kramers–Kronig analysis.

The authors gratefully acknowledge the financial support of Asahi Glass Co., Ltd.

References

1. J. P. Hawranek, P. Neelakantan, R. P. Young, and R. N. Jones, "The control of errors in IR spectrophotometry. IV. Corrections for dispersion distortion and the evaluation of both optical constants," Spectrochim. Acta Part A **32,** 85–98 (1976).
2. J. P. Hawranek and R. N. Jones, "The control of errors in IR spectrophotometry. V. Assessment of errors in the evaluation of optical constants by transmission measurements on thin films," Spectrochim. Acta Part A **32,** 99–109 (1976).
3. J. P. Hawranek, and R. N. Jones, "The determination of the optical constants of benzene and chloroform in the IR by thin film transmission," Spectrochim. Acta Part A **32,** 111–123 (1976).
4. G. K. Ribbegård and R. N. Jones, "The measurement of the optical constants of thin solid films in the infrared," Appl. Spectrosc. **34,** 638–645 (1980).
5. R. T. Graf, J. L. Koenig, and H. Ishida, "Optical constant determination of thin polymer films in the infrared," Appl. Spectrosc. **39,** 405–407 (1985).
6. F. Wooten, "Dispersion relations and sum rules," *Optical Properties of Solids* (Academic, New York, 1972), Chap. 6.
7. D. G. Cameron, D. Escolar, T. G. Goplen, A. Nadeau, R. P. Young, and R. N. Jones, "A reflection spectrophotometer for the measurement of the optical constants of liquids in the infrared," Appl. Spectrosc. **34,** 646–651 (1980).
8. T. G. Goplen, D. G. Cameron, and R. N. Jones, "The control of errors in infrared spectrophotometry. VI. The evaluation of optical constants by combined transmission and attenuated total reflection measurements," Appl. Spectrosc. **34,** 652–656 (1980).
9. T. G. Goplen, D. G. Cameron, and R. N. Jones, "Absolute absorption intensity and dispersion measurements on some organic liquids in the infrared," Appl. Spectrosc. **34,** 657–691 (1980).
10. J. E. Bertie and H. H. Eysel, "Infrared intensities of liquids. I. Determination of infrared optical and dielectric constants by

FT-IR using the CIRCLE ATR cell," Appl. Spectrosc. **39,** 392–401 (1985).
11. J. E. Bertie, S. L. Zhang, and R. Manji, "Infrared intensities of liquids. X. Accuracy of current methods of obtaining optical constants from multiple attenuated total reflection measurements using the CIRCLE cell," Appl. Spectrosc. **46,** 1660–1665 (1992).
12. T. S. Robinson, "Optical constants by reflection," Proc. Phys. Soc. London Sect. B **65,** 910–911 (1952).
13. T. S. Robinson and W. C. Price, "The determination of infra-red absorption spectra from reflection measurements," Proc. Phys. Soc. London Sect. B **66,** 969–974 (1953).
14. J. S. Plaskett and P. N. Schartz, "On the Robinson–Price (Kramers–Kronig) method of interpreting reflection data taken through a transparent window," J. Chem. Phys. **38,** 612–617 (1963).
15. D. M. Roessler, "Kramers–Kronig analysis of reflection data," Br. J. Appl. Phys. **16,** 1119–1123 (1965).
16. D. M. Roessler, "Kramers–Kronig analysis of non-normal incidence reflection," Br. J. Appl. Phys. **16,** 1359–1366 (1965).
17. D. W. Berreman, "Kramers–Kronig analysis of reflectance measured at oblique incidence," Appl. Opt. **6,** 1519–1521 (1967).
18. G. M. Hale, W. E. Holland, and M. R. Querry, "Kramers–Kronig analysis of relative reflectance spectra measured at an oblique angle," Appl. Opt. **12,** 48–51 (1973).
19. M. R. Querry and E. Holland, "Kramers–Kronig analysis of ratio reflectance spectra measured at an oblique angle," Appl. Opt. **13,** 595–598 (1974).
20. A. H. Kachare, W. G. Spitzer, F. K. Euler, and A. Kahan, "Infrared reflection of ion-implanted GaAs," J. Appl. Phys. **45,** 2938–2946 (1974).
21. E. G. Makarova and U. N. Morozov, "Calculation of the phase spectrum using the Kramers–Kronig relationships," Opt. Spectrosc. (USSR) **40,** 138–140 (1976).
22. R. E. Prange, H. D. Drew, and J. B. Restorff, "Analysis of Kramers–Kronig relations in modulation spectroscopy," J. Phys. C **10,** 5083–5088 (1977).
23. R. Young, "Validity of the Kramers–Kronig transformation used in reflection spectroscopy," J. Opt. Soc. Am. **67,** 520–523 (1977).
24. J. A. Bardwell and M. J. Dignam, "Extensions of the Kramers–Kronig transformation that cover a wide range of practical spectroscopic applications," J. Chem. Phys. **83,** 5468–5478 (1985).
25. J. A. Bardwell and M. J. Dignam, "Routine determination of the absorption and dispersion spectra of solids with a Fourier-transform infrared spectrometer," Anal. Chim. Acta **172,** 101–110 (1985).
26. J. A. Bardwell and M. J. Dignam, "Routine method for the determination of the optical constants of liquids," Anal. Chim. Acta. **181,** 253–258 (1986).
27. B. Harbecke, "Application of Fourier's allied integrals to the Kramers–Kronig transformation of reflectance data," Appl. Phys. **40,** 151–158 (1986).
28. K. Jezierski, "Improvements in the Kramers–Kronig analysis of reflection spectra," J. Phys. C **19,** 2103–2112 (1986).
29. M. J. Dignam and S. Mamiche-Afara, "Determination of the spectra of the optical constants of bulk phases via Fourier transform ATR," Spectrochim. Acta. Part A **44,** 1435–1442 (1988).
30. M. J. Dignam, "Fourier transform polarization spectroscopy," Appl. Spectrosc. Rev. **24,** 99–135 (1988).
31. K. Yamamoto and A. Masui, "Kramers–Kronig analysis of FT-IR normal reflection spectra and spectral simulation using complex refractive index," presented at Euroanalysis VII, Vienna, 26–31 August, 1990.
32. R. M. A. Azzam and N. M. Bashara, "Reflection and transmission of polarized light by stratified planar structures," *Ellipsometry and Polarized Light.* (North-Holland, Amsterdam, 1987), Chap. 4.
33. F. Wooten, "Absorption and dispersion," *Optical Properties of Solids.* (Academic, New York, 1972), Chap. 3.
34. J. A. Bardwell and M. J. Dignam, "Fourier transform polarimetry," in *Polymer Science and Technology,* H. Ishida, ed. (Plenum, New York, 1987), pp. 415–433.